Thin-Film Behavior of Poly(methyl methacrylates). 2. An FT-IR Study of Langmuir-Blodgett Films of Isotactic PMMA

R. H. G. Brinkhuis and A. J. Schouten*

Department of Polymer Chemistry, University of Groningen, Nijenborgh 16, 9747 AG Groningen, The Netherlands

Received June 22, 1990; Revised Manuscript Received September 6, 1990

ABSTRACT: The structure of Langmuir-Blodgett films of isotactic PMMA transferred to substrates was investigated with FT-infrared techniques. From the results it is argued that at high surface pressures, the isotactic PMMA is transferred in a crystalline-like conformation, presumably as double helices. The films built of this type of Langmuir-Blodgett layers can easily be crystallized further, in contrast with films of amorphous isotactic PMMA. Infrared techniques were also used to deduce the orientational characteristics of the crystalline structures. These were found to be strongly dependent on the molecular weight and monolayer history. Very strongly oriented, highly crystalline thin films could be prepared starting from Langmuir-Blodgett multilayers.

Introduction

Since the introduction of the Langmuir-Blodgett technique to prepare organized multilayer assemblies of organic substances, much effort has been devoted to the optimization of the processes and the physical characterization of the monolayer and multilayer films prepared this way. The Langmuir-Blodgett technique proved to be a very powerful tool for preparing thin films, in the first place because of the well-defined deposition characteristics, allowing the preparation of thin films with a well-defined homogeneous thickness. This aspect of the LB technique is very important with respect to possible applications of the thin films as spacer layers or for use in areas like microlithography.[1]

Another very important feature of the thin films prepared by the Langmuir-Blodgett technique is the fact that the molecules may be present in the multilayers in an ordered structure (sometimes a crystalline structure, as is found for many amphiphilic molecules with long hydrocarbon tails[2-6]), with very distinct orientational characteristics. The enhanced thermal stability induced by the crystallinity and the orientation of the molecules imply interesting possibilities for optical applications,[7,8] whereas the ordered structures may also serve as models for biological systems.[9]

It is obvious that the characterization of the structure is a very important aspect of the study of LB multilayer systems. Many techniques are available, the most widespread being X-ray diffraction, ellipsometry, and IR spectroscopy. The latter technique is probably the most versatile and has been used by many workers,[2-6,10-15] especially since the commercial introduction of FT-IR instruments. Infrared spectroscopy has the capability to reveal various conformational features and can also be used to determine the orientation of parts of the molecules directly.

Several IR techniques can be used to investigate thin films prepared by the LB technique. External reflection spectroscopy (also referred to as grazing incidence reflection or as reflection absorption spectroscopy) is commonly used for thin films on reflecting metal substrates. Since Francis and Ellison[16] studied metal stearate films using this technique and Greenler[17] discussed the optics involved, many authors have used this technique for studying Langmuir-Blodgett films.[3-6,10,13,14] Since upon reflection on the metal surface the resulting electrical field is strongly elliptically polarized, with only a significant contribution of the component perpendicular to the surface, the orientation of the molecules with respect to the surface can be inferred. Other IR techniques that can be used to deduce the orientation of the thin film include transmission experiments on IR-transparent substrates[5,10,11] and attenuated total reflection measurements as used, e.g., by Takenaka,[12] using polarized IR radiation. A completely different approach to elucidate the orientation of LB films was reported by Chatzi et al. using a photoacoustic technique with He and Xe coupling gases.[18]

In the preceding paper[19] we have reported on the monolayer behavior of stereoregular poly(methyl methacrylates), especially of isotactic PMMA. In this paper, we describe an IR study of thin films made from Langmuir-Blodgett multilayers of isotactic PMMA, using transmission and external reflection techniques.

Experimental Section

Materials. PMMA samples were synthesized and characterized as described in ref 19. Triad tacticities and molecular weight characteristics are listed in Table I of ref 19. Unless stated otherwise, the isotactic PMMA fraction used was sample 5, having a molecular weight ($\bar{M}_n$) of 36 000.

Substrates for the external reflection IR measurements were prepared by argon plasma sputtering of gold (approximately 800-Å thickness) onto a microscope slide. For transmission IR experiments ZnS substrates (2-mm-thick Cleartran) were used.

Langmuir-Blodgett layers were transferred to the substrates by a vertical dipping method. The transfer pressure was allowed to stabilize for at least 45 min. The dipping speed was 4 mm/min, and the operating temperature was 22 °C unless stated otherwise.

Apparatus. The Langmuir troughs used to prepare the LB films are described in the previous publication.[19]

Infrared measurements were performed with a Bruker IFS88 FTIR spectrophotometer equipped with a MCT-A D-313 detector. A germanium Brewster angle IR polarizer was used for both grazing angle reflection and transmission experiments. Grazing angle reflection spectra were recorded in 80° specular setup with light polarized parallel to the plane of incidence and referenced against the reflection spectrum of a clean gold layer.

Thin-film transmission experiments were performed under a small (5°) tilt in order to avoid problems with internal reflections within the ZnS substrate. Simulation of IR transmission spectra indicated that this tilt would not result in a significant change in the spectra as compared to a zero angle of incidence. Transmission spectra of the bare substrates were used as reference spectra. All spectra were recorded at 4-cm^{-1} resolution, and 1000-2000 scans (both sample and reference side) were averaged.[10] All reported spectra were baseline corrected.

0024-9297/91/2224-1496$02.50/0

Spectral Simulations. Transmission and reflection IR spectra were simulated by using PMMA optical constants estimated according to the following procedure. A transmission spectrum of an approximately 2-μm-thick cast amorphous film (heated to 170 °C to remove all order possibly present) on KBr (which ensures a low level of optical distortions due to the dispersion of the real part of the refractive index) was used as an "input" spectrum. The absolute values for the imaginary part of the refractive index were estimated by evaluating transmission spectra of free-standing films of the same material. The real part of the refractive index was subsequently calculated from its imaginary part by a Kramers–Kronig transformation. For all PMMA samples this real part of the refractive index was centered at 1.43.[20] The Kramers–Kronig transformation was performed numerically with a step size of 1 cm^{-1}, using an approach based on MacLaurin's formula, which yields the most accurate results according to Ohta and Ishida.[21] The results obtained this way could satisfactorily reproduce transmission spectra of free-standing films and agree well with those published by Graf and Ishida.[20]

Reflection and transmission spectra of thin films were calculated from these optical constants by using the matrix approach introduced by Abelés.[22] For the optical constants of the substrates complex refractive index values were used of $9.5 - 30i$ for gold[23] and 2.22 for ZnS[24] over the entire IR range studied.

Results and Discussion

The results discussed in this article are closely related to those reported in the previous paper,[19] in which the monolayer behavior of isotactic PMMA at the air–water interface was studied. In this article we will focus on the FT-IR study of the structure and the behavior of Langmuir–Blodgett films transferred to substrates with FT-IR techniques.

The first problem to be solved was the nature of the transition observed in the pressure–area isotherm of isotactic PMMA at a specific area of approximately 20 $Å^2$/monomeric unit.[19] Therefore the infrared spectra of films transferred at surface pressures below and above the transition pressure (5 and 12 mN/m, respectively) were recorded.

The grazing angle infrared reflection spectra of Langmuir–Blodgett layers of isotactic PMMA transferred with a surface pressure of 5 mN/m is shown in Figure 1C, together with the IR bulk transmission spectrum of amorphous isotactic PMMA (Figure 1A), the calculated grazing incidence reflection spectrum of amorphous nonoriented isotactic PMMA (Figure 1B; for more details we refer to the Experimental Section), and a GIR spectrum of a thin layer of isotactic PMMA that was heated to 170 °C (above the T_g and the T_m) to remove all possibly remaining order and orientation. Because of the high absorption coefficients of PMMA, the GIR spectra will be severely distorted as compared to ordinary transmission spectra (as is evident from a comparison of parts A and B of Figure 1), and therefore it is necessary to calculate the reflection spectrum of an amorphous film in order to have a reference spectrum to compare with the experimental spectra. In this thickness regime the shape of the spectrum (apart from its absolute intensity) does not depend on film thickness, an observation that is confirmed experimentally.

Comparing the experimental GIR spectrum of the multilayer formed by transfer at a surface pressure of 5 mN/m (Figure 1C) with the simulated spectrum based on a film of amorphous isotactic PMMA, we see that these spectra are almost identical. So, from these GIR spectra there are no indications that the structure of the multilayer deviates from an amorphous bulk structure. A thin film of isotactic PMMA (approximately 150 Å), heated to 170 °C (assumed to be completely amorphous), yields a GIR

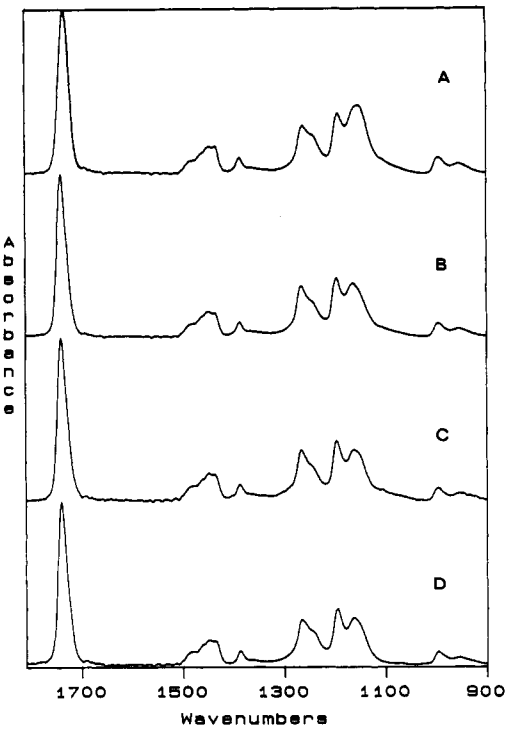

Figure 1. IR spectra of isotactic PMMA: (A) Bulk transmission spectrum of amorphous PMMA; (B) simulated GIR spectrum of a 200-Å film of isotactic PMMA on gold; (C) GIR spectrum of an "as-deposited" multilayer of isotactic PMMA transferred at a surface pressure of 5 mN/m; (D) GIR spectrum of a thin film of isotactic PMMA on gold after heating to 170 °C.

spectrum practically identical with the 5 mN/m multilayer and the calculated amorphous spectrum (Figure 1D). Probably, during transfer at low surface pressures, the monolayer chains are deposited in a more or less random manner, the polymer structures being rather flexible in the "expanded" condition of the monolayer.[19]

On the other hand, the spectrum that is recorded from a multilayer transferred by using a surface pressure of 12 mN/m (approximately 150 Å, assuming a normal density) deviates significantly from the calculated spectrum of amorphous isotactic PMMA. This is shown in Figure 2A. The features that distinguish this spectrum from the calculated amorphous spectrum include in the first place a strong difference in the intensity of the overlapping bands at 1265 and 1255 cm^{-1} (which have been reported to be conformation sensitive).[25-27] Other deviations that may be less obvious include a shoulder emerging at 1296 cm^{-1}, a "sharpening" of the broad 1154-cm^{-1} band, some changes in the C–H bending vibrations around 1440 cm^{-1}, and in the α-methyl and methylene C–H rocking vibrations at 950 and 840 cm^{-1}, respectively. The C–H stretching region (2800–3100 cm^{-1}, not shown in Figure 2) also exhibits some differences. See also Table I.

For all these observed deviations, similar differences can be observed upon comparing a bulk spectrum of amorphous isotactic PMMA with that of crystalline isotactic PMMA. This can be seen in Figure 2, where simulated GIR spectra based on optical constants derived from bulk spectra of amorphous and crystalline i-PMMA are drawn. Also, when (partially) deuterated isotactic PMMA samples are used (α-methyl CD_3, ester methyl CD_3, backbone CD_2, and totally deuterated D_8), it can be seen that the grazing incidence reflection spectra of multilayers transferred at 12 mN/m surface pressure deviate from the calculated GIR spectra of the amorphous material and that again all deviations can be traced back to similar differences between bulk spectra of amorphous and

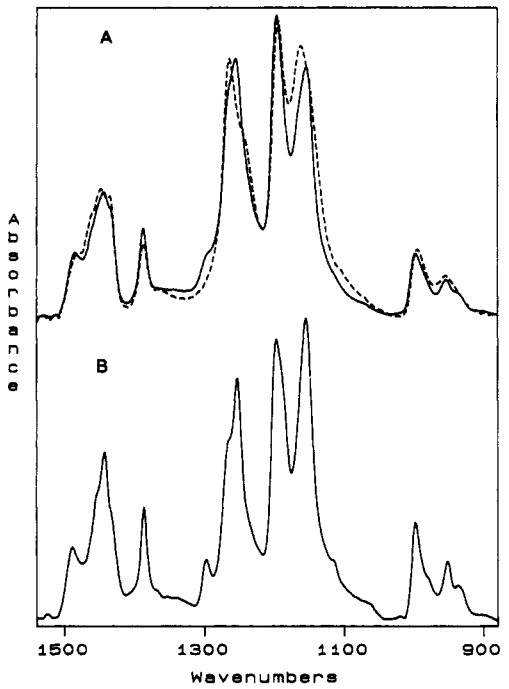

Figure 2. (A) GIR spectrum of an "as-deposited" multilayer of isotactic PMMA, transfer pressure 12 mN/m (—); simulated GIR spectrum for a thin film of amorphous i-PMMA on gold (- - -). (B) Simulated GIR spectrum of a thin film of isotropic crystalline i-PMMA on gold.

Table I
Assignments of Relevant IR Absorption Bands of Isotactic PMMA[a]

wavenumber, cm^{-1}	assignment
2995	α-CH_3 asym str, OCH_3 asym str
2958	α-CH_3 sym str, OCH_3 sym str, CH_2 str
2930	CH_2 str
1734	C=O sym str
1483	α-CH_3 asym bend
1465	OCH_3 asym bend
1448	CH_2 scissor bend
1445	OCH_3 sym str
1388	α-CH_3 sym bend
1296	delocalized, containing mostly backbone and methylene vibrations;[31] characteristic for crystalline i-PMMA
1265	out-of-phase asym C–C–O stretch, coupled with CH_2
1255	in-phase asym C–C–O stretch, coupled with CH_2
1190	no clear assignments; possibly C–O–C str
1150	combination of delocalized modes of various ester vibrations and CH_2 rocking modes
996	OCH_3 rocking
951	α-CH_3 rocking
842	not clear; probably CH_2 rocking

[a] Assignments of some bands are still a subject of debate.[28]

crystalline samples of these materials (not shown here). We can conclude that the structure of the isotactic PMMA in these multilayers has definite crystalline characteristics.

The structure of crystalline isotactic PMMA has been the subject of some debate, but it is now generally accepted to be a 10/1 double helix.[29-31] Because of the similarity between the infrared characteristics of multilayers transferred at 12 mN/m and bulk crystalline material, it is likely that the isotactic PMMA is transferred to the substrate in similar double-helical structures. This hypothesis proved to be very useful in explaining the results from the monolayer study reported in the accompanying paper and is also in agreement with the results reported later in this paper.

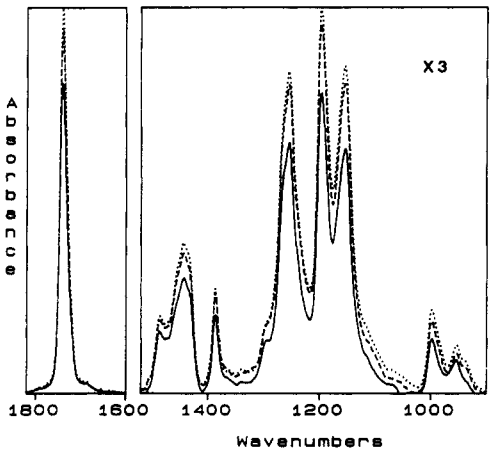

Figure 3. GIR spectra for an "as-deposited" multilayer of isotactic PMMA (transfer pressure 12 mN/m) (···) and after heating to 55 °C for 14 h (- - -), and 70 °C for 2 h (solid line). The spectra are shown on the same scale.

The reflection spectrum of the 12 mN/m multilayer is not identical with a calculated reflection spectrum based on a bulk transmission spectrum of crystalline isotactic PMMA as can be seen in Figure 2. Partly this is caused by fact that the Langmuir–Blodgett structures are oriented with respect to the substrate, which causes dichroic effects to be observed in the GIR spectrum; we will elaborate on this subject later in this article. Apart from dichroic effects, the crystalline features are also less pronounced in the "as-deposited" multilayer spectrum compared to the spectrum of bulk crystalline material. This may be caused not only by a significant fraction of amorphous material present but also by the absence of a three-dimensional crystalline packing of the crystalline subunits (the helices). A crystalline packing will be very difficult to achieve directly, depositing rigid structures layer by layer from the water surface onto the substrate, especially since the LB layers do not exhibit a perfect X, Y, or Z type transfer. The "loose" structure anticipated this way (and discussed later in this article) may have less well pronounced crystalline IR characteristics as compared to the same structures in a really crystalline packing.

We will further focus on the behavior of multilayers deposited at 12 mN/m.

When the "high surface pressure" (12 mN/m) multilayers are heated to above the T_g of the isotactic PMMA (approximately 50 °C), the anomalous features (as compared to the amorphous spectrum) do not disappear from the GIR spectrum: the deviating structure does not relax by heating it to above the normal T_g (the shape of the spectrum hardly changes), which is another indication that we are dealing with crystalline-like structures. What we do see is a decrease in the IR absorption of the film over the whole spectrum upon annealing above T_g. This is shown in Figure 3.

This decrease of the absorption intensity may be related to variations in the density of the films as is discussed in Appendix 1. It can be explained by an increase in the density of the polymer film upon annealing above T_g: the loose structure of the as deposited multilayer collapses. Ellipsometry experiments confirmed the low density of the "as-deposited" multilayers relative to the normal bulk density. For multilayers transferred at low surface pressures (e.g., 5 mN/m) and heated to temperatures far above the T_g, a GIR intensity is found that does not deviate strongly from the "as-deposited" thin film, indicating a similar density.

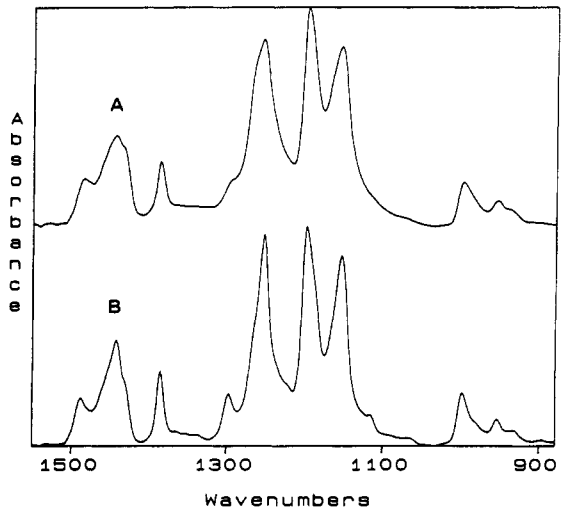

Figure 4. (A) GIR spectrum of an "as-deposited" multilayer of isotactic PMMA on gold (transfer pressure 12 mN/m). (B) GIR spectrum of the same thin film after being heated for 3 days at 120 °C.

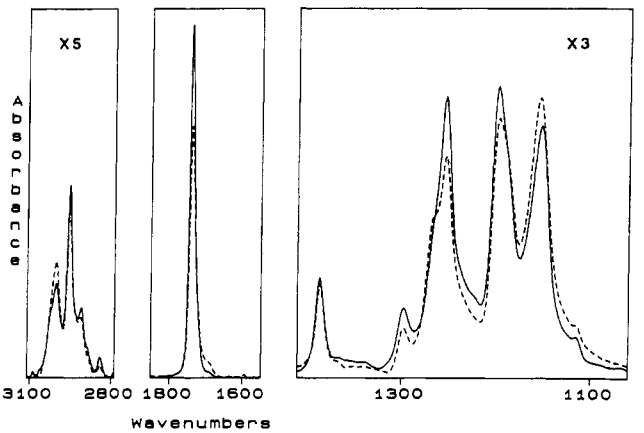

Figure 5. Experimental GIR spectrum of a crystallized LB multilayer (compare Figure 9) (—) and the calculated GIR spectrum for a crystalline thin film of the same thickness (145 Å, - - -). The spectra are plotted on the same scale.

Multilayer Crystallization. When we anneal the multilayers that were transferred at a 12 mN/m surface pressure, at 120 °C, we see a rapid change in the GIR infrared spectrum: the crystalline features get more and more pronounced (Figure 4) to a similar extent (or even more) as those in the bulk spectrum of crystalline isotactic PMMA. The pseudocrystalline structure of the Langmuir–Blodgett multilayer is converted into a "real" three-dimensionally packed crystalline structure. Similar multilayers consisting of partially deuterated materials exhibit identical behavior: upon annealing at 120 °C they attain a crystalline structure similar to that in the bulk, as evidenced by the IR spectra.

The relative peak ratios in the GIR spectrum of the crystallized multilayers are not identical with those in the spectrum calculated for a film of the same thickness, based on the optical constants derived from an isotropic crystalline bulk sample; in fact the deviations are quite strong (compare Figure 5). The intensities of, e.g., the C=O stretching vibration (1740 cm^{-1}), the α-methyl C–H symmetric bending vibration at 1390 cm^{-1}, and absorption bands at 2958 and 1255 cm^{-1} are too high relative to the simulated spectrum, whereas, e.g., the bands at 3000 and 1265 cm^{-1} are too low. These dichroic effects are similar to those observed in the spectra of the "as-deposited" films, only much clearer now. The dichroic effects can be explained if we assume that the helical structures are

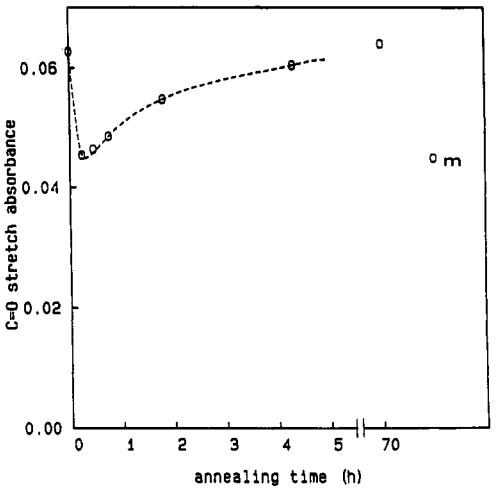

Figure 6. Intensity of the C=O stretch absorbance for a multilayer of isotactic PMMA transferred at 12 mN/m, as a function of the annealing time at 120 °C. The 0-h data point corresponds to the "as-deposited" film. m: value for the same film after heating to 170 °C.

oriented parallel with respect to the substrate (and also more or less did so in the as-deposited layer). Such an orientation can be expected for helices that are transferred layer by layer from the water surface. Appendix 2 gives a short discussion of the dichroic effects that can be calculated for this situation. Assuming a ϕ (angle between transition dipole moment and helix axis) larger than 55° for the C=O stretching and the α-CH_3 symmetric C–H bending vibrations, as can be inferred from the proposed crystal structure of isotactic PMMA,[30] a relative increase of the absorption bands associated with these vibrations can be anticipated.

The crystallization of the multilayer is a relatively very rapid process, compared to bulk crystallization kinetics. Already after it is annealed for 5 min, significant changes toward the "real" crystalline structure are observable in the GIR spectrum. We can use, e.g., the maximum absorption intensity of the C=O stretching vibration to follow the processes in the multilayer upon annealing at 120 °C. An example is given in Figure 6, in which this intensity is plotted versus the annealing time. The data point at $t = 0$ corresponds to the value of the as-deposited multilayer. Upon annealing, the absorption intensity first drops very sharply (approximately 25%), due to the collapse of the loose as-deposited structure of the multilayer into a more dense packing.

Subsequently the intensity of the 1740-cm^{-1} band starts to increase rapidly and levels off in a few hours. When the film is heated to 170 °C, the GIR spectrum loses its crystalline features, and the film attains an amorphous, randomly oriented structure. Correspondingly, the C=O absorption intensity drops sharply.

The enhancement of the dichroic features of the crystalline isotactic PMMA as compared to the presumably pseudocrystalline as-deposited structure of the film can be caused by an increase in the helix content, or by an enhanced orientation of the helices present along the average direction of the entire film structure, but also by the fact that a three-dimensional packing of the helices, which is probably not obtained until annealing at 120 °C, may force the side groups into a fixed position and orientation with respect to the helix. If the absence of a crystalline packing of the helices would allow the side groups a higher mobility, this would also tend to diminish the dichroic effects.

The observation that the isotactic PMMA, deposited at high surface pressures, can easily attain a highly crystalline structure is striking when it is compared to the normal crystallization characteristics of this material. Isotactic PMMA normally crystallizes notoriously slowly, even at 120 °C, which is considered the optimal crystallization temperature.[32,33] Even for rather favorable molecular weights it may take days for crystallization to be observed either by IR (2-μm-thick films cast on KBr) or differential scanning calorimetry (DSC). With increasing molecular weight of the isotactic PMMA the crystallization rate even slows down further rapidly, so that crystallization of these higher molecular weight fractions is very time-consuming.[34] In contrast, high molecular weight fractions (we studied molecular weights up to 10^6) of isotactic PMMA deposited at a surface pressure of 12 mN/m to form a multilayer can very easily crystallize similarly to the $\bar{M}_n$ 36 000 material used for the films from Figure 4.

The ease of crystallization of isotactic PMMA films prepared this way becomes even more remarkable when we compare it to the behavior of amorphous thin films with similar thicknesses of up to several hundreds of angstroms. Because of the restricted geometry of the thin film, crystallization will be severely suppressed with respect to bulk samples,[35] which leads to the observation that thin films of amorphous isotactic PMMA (transferred at low surface pressures or after being heated to 170 °C) do not crystallize significantly even after 1 month at 120 °C (not even the fractions with rather favorable molecular weights).

As expected, isotactic PMMA of low molecular weight ($\bar{M}_n$ 2800, sample 16[19]) that did not form the proposed helical structures on the water surface could not be crystallized after transfer at 12 mN/m surface pressure.

Melting Behavior. The melting behavior of the crystallized multilayers was studied by heating the film to a certain temperature and subsequently recording a GIR IR spectrum to evaluate the crystallinity. To compare the melting point to that of a bulk crystalline sample, IR transmission spectra were also taken from a 2-μm-thick crystalline film on KBr after simultaneous heating. The melting region for the "bulk" film was thus found to be 156–164 °C, which corresponds well with DSC experiments. The crystallized LB film loses its crystallinity starting at significantly lower temperatures, the melting region expanding somewhere from 140 to 155 °C, depending on the layer thickness. For the thicknesses studied (up to 300 Å) the melting region was significantly lower than that of corresponding bulk crystalline films.

The reason for this difference may be in the first place the nucleation density, which can be anticipated to be higher for the crystallized multilayer because of the presence of a large number of potential nuclei (the helices as transferred from the water surface), possibly leading to small crystallites compared to the more extensive lamellar structures formed in conventional melt crystallization. On the other hand, the crystallite size will also be limited by the thickness of the film, prohibiting large crystallites to be formed. An indication that this latter phenomenon is significant is illustrated by the observation that very thin films (up to approximately 60 Å at normal density) do not crystallize upon annealing at 120 °C but instead lose the (pseudo) crystalline features present in the "as-deposited" film. Probably, these films are too thin for crystallites to be formed that are large enough to be stable at the crystallization temperature. Also when studying the melting region of crystalline films of varying thicknesses (above the apparent crystallization treshold), we observed that upon increasing the film thickness, the melting range tends to shift somewhat to higher temperatures. This effect is still being studied in more detail in our laboratory.

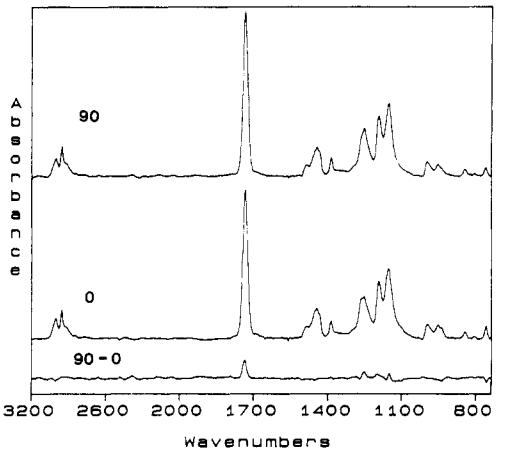

Figure 7. Polarized transmission spectra of an "as-deposited" multilayer of isotactic PMMA (sample 5, $\bar{M}_n$ 36 000, transfer pressure 12 mN/m) and the difference spectrum. Polarization direction is indicated in the figure. All spectra are shown on the same scale.

Lateral Orientation. Apart from GIR experiments, reported above, we also carried out transmission experiments with multilayers transferred to IR-transparent substrates. This allows the film to be probed by an electrical field parallel to the substrate, with the possibility of distinguishing the dipping (transfer) direction from the direction perpendicular to it by using polarized light. We will refer to the polarization parallel to the dipping direction as 0° and perpendicular to this dipping direction as 90°.

When a 300-Å-thick multilayer of isotactic PMMA ($\bar{M}_n$ 36 000) on a ZnS substrate, transferred at a pressure of 12 mN/m, is studied, we see that the transmission spectra obtained without polarization confirm the dichroic effects observed in the GIR spectra, the relative band ratios being oppositely affected. Performing transmission experiments with polarized IR radiation, we find that the spectrum obtained with 0° polarization is not identical with the spectrum obtained by using a 90° polarization (Figure 7). The same type of dichroic effects are observed as in the GIR spectra (Figure 5; the same bands are affected, as will be clearer later on); e.g., the 1732-cm^{-1} absorption band is stronger in the spectrum obtained with 90° polarization than in the spectrum obtained with the 0° polarization. (The difference in the position of the C=O stretching vibration is merely an optical effect, which also follows from the spectral simulations.)

For the GIR spectra we argued that the relatively high intensity of the carbonyl band was caused by the fact that the angle of the carbonyl stretching dipole transition moment with the helix axis was larger than 55°, resulting in a higher absorption value for IR radiation polarized in a direction perpendicular to the helix axis than for a polarization along the helix axis (Appendix 2). The observation that light polarized perpendicular to the dipping direction is absorbed more strongly by the carbonyl dipole than radiation polarized parallel to this dipping direction indicates that the helices are preferentially oriented in the dipping direction. A similar orientation of helical structures in the transfer direction was reported by several authors.[15,36,37]

This lateral orientation of the helical structures of isotactic PMMA must be caused by the flow that occurs at the meniscus between the substrate and the water surface

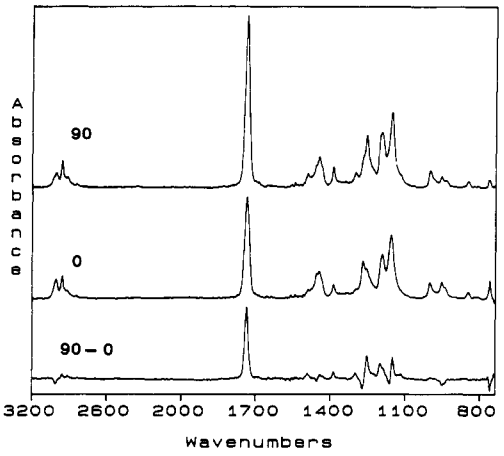

Figure 8. Polarized transmission spectrum of the film from Figure 7, after crystallization for 3 days at 120 °C, and the difference spectrum. Polarization direction is indicated in the figure. All spectra are shown on the same scale.

during dipping. A 90° rotation of the substrate with respect to the barrier (substrate surface perpendicular to the moving barrier instead of parrallel to it) produces the same results, indicating that the lateral orientation observed is not caused by a preferential orientation in the monolayer on the water surface due to the direction of the movement of the moving barrier.

To quantitatively discuss this lateral orientation effect, we here introduce a lateral orientation parameter L defined as

$$L_x = \frac{I_{90} - I_0}{I_{90} + I_0}$$

in which I_{90} and I_0 represent the absorption intensities of band x using light polarized perpendicular and parallel to the dipping direction, respectively. For the case that all the helices are oriented parallel to the substrate, it can easily be shown that depending on the lateral orientation in the XY plane this value can vary in theory between 1 and −1, these values being able to be reached only by absorption bands associated with dipole transition moments with $\phi = 0°$ or $\phi = 90°$, intermediate values of ϕ leading to smaller (absolute) asymptotic values. For the C=O stretching vibration, with a ϕ larger than 55° positive values for this parameter indicate a preferential lateral orientation of the helical structures parallel to the dipping direction, negative values to a preference perpendicular to the dipping direction. For the spectra of Figure 7 an $L_{C=O}$ value of 0.07 can be calculated.

When the "as deposited" multilayer (transfer pressure 12 mN/m) is heated to 70 °C (above T_g), we observe (as in the GIR experiments) that the anomalous crystalline characteristics are retained. The $L_{C=O}$ value does not change very much (from 0.07 to 0.09), and the absorption intensity of the spectra with both polarizations increases slightly due to densification of the film.

Upon annealing at 120 °C, the effect of the crystallization process can also be observed in the transmission spectra (Figure 8). The crystalline features in the spectrum are much more pronounced than for the as-deposited film, but the most striking observation is the difference between the spectra with different polarizations. As in the GIR spectrum the dichroic effects are enhanced upon crystallization. The $L_{C=O}$ value for the crystallized film is 0.26, indicating a fairly strong orientation of the helices in the original dipping direction. Similar to the GIR spectra, the increase of this value upon crystallization may be explained by a reorientation of the helices to a common

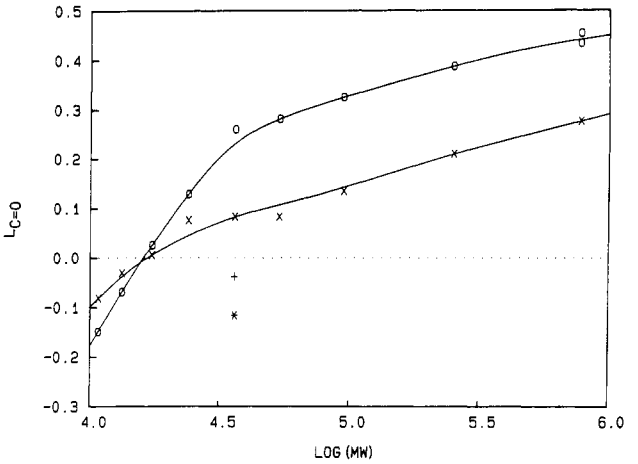

Figure 9. $L_{C=O}$ values as a function of the molecular weight of the isotactic PMMA: (×) "as-deposited", stabilization at 12 mN/m; (○) the same films after crystallization at 120 °C; (+) as-deposited, stabilization at 6.5 mN/m; (*) the same film, after crystallization at 120 °C.

average direction (since the helices must be parallel for a crystalline packing) as well as by a decrease of the mobility of the side groups in the "as-deposited" multilayer without a real three-dimensional packing, obscuring dichroic effects. The spectrum obtained by subtracting the 90° and 0° spectra illustrates the dichroic effects observed; the agreement of the dichroic effects in the GIR spectra and the transmission spectra can easily be checked. When the crystalline multilayer is heated to 170 °C, all crystalline spectral features and all orientation effects disappear from the transmission spectra.

An increase of the dipping speed from 4 to 16 mm/min did not affect the lateral orientation: both the "as-deposited" film and the crystallized film yielded similar L values.

When a multilayer was built by transferring isotactic PMMA with a low molecular weight ($\bar{M}_n$ 2800, sample 16, not being able to form the proposed helical structures on the water surface[19] at 12 mN/m, the "as-deposited" films, as well as the films that were annealed at 120 °C, exhibited no lateral orientation, as was expected. For Langmuir–Blodgett films, prepared by transfer of the isotactic PMMA at low surface pressures, from an expanded monolayer condition, no clear lateral orientation effects could be inferred from the polarized transmission experiments either. The 90° and 0° spectra are practically identical.

Lateral Orientation vs Molecular Weight. The lateral orientation of the 12 mN/m transferred multilayers exhibits a very remarkable dependence on the molecular weight of the isotactic PMMA. This is illustrated in Figure 9, in which the $L_{C=O}$ values are reported for the multilayers (all approximately 300 Å thick) both as-deposited and after crystallization at 120 °C. We see that in all cases the lateral orientation is enhanced by the crystallization process.

With increasing molecular weight of the isotactic PMMA the value for the lateral orientation parameter $L_{C=O}$ increases consistently, both for the "as-deposited" and for the crystallized films. The use of high molecular weight fractions produces multilayers in which the preference for the helices parallel to the dipping direction becomes very strong, especially after crystallization: for the crystalline films of the highest molecular weight fraction this results in an increase of a factor of more than 2.5 in the intensity of the C=O absorption upon going from 0° to 90° polarized light. The spectra for this film are shown in Figure 10. A comparison of these spectra with the GIR

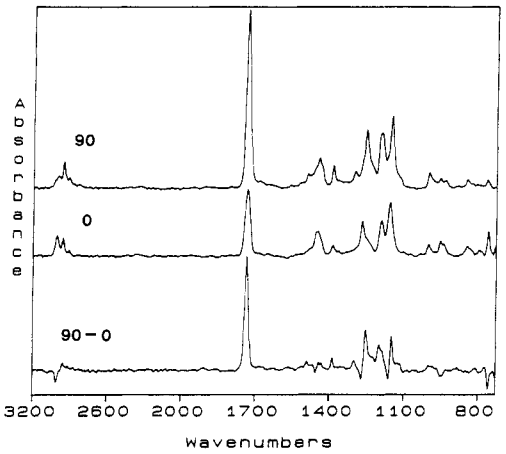

Figure 10. Polarized transmission spectra of a multilayer of isotactic PMMA (sample 1, $\bar{M}_n$ 770 000, transfer pressure 12 mN/m), crystallized for 3 days at 120 °C, and the difference spectrum. Polarization direction is indicated in the figure. All spectra are shown on the same scale.

spectra indicates that the preference of the helices for the direction parallel to the dipping direction approaches that for the direction parallel to the substrate. The dichroic effects in these spectra even seem to be significantly larger than those in the polarized IR spectra of isotactic PMMA, crystallized after being uniaxially stretched up to a draw ratio of 10–15, as reported by Dybal and Krimm.[31]

Lowering the molecular weight of the isotactic PMMA results in a decrease of the $L_{C=O}$ value, which becomes 0 at molecular weights of about 15 000. For these materials there is no preference for either direction in the XY plane. Lowering the molecular weight even further (without entering the regime where the isotactic PMMA no longer forms the suggested helical structures on the water surface[19]) results in *negative* values for the $L_{C=O}$, indicating a preferential orientation of the helices *perpendicular* to the dipping direction.

The same reversal of the preferred helix direction was observed by using the $\bar{M}_n$ 36 000 isotactic PMMA, after the monolayer was stabilized at the water surface at a low surface pressure (6.5 mN/m, instead of the normal procedure of stabilizing the film immediately at 12 mN/m). When this monolayer was subsequently transferred to the substrate at a surface pressure of 12 mN/m, a negative value for $L_{C=O}$ is found (−0.04 for the "as-deposited" film and −0.12 for the crystallized film), again indicating a preferential orientation perpendicular to the dipping direction.

Increasing the molecular weight of the isotactic PMMA will probably increase the monolayer viscosity and thus modify the shear forces that may orient the rigid helical structures in the flow associated with the dipping procedure. This argument alone does not suffice though, because it cannot explain why the preferential orientation can be inverted by using low molecular weight samples or lower stabilization surface pressures.

To explain these effects, we return to the crystallization process suggested for the transition in the monolayer on the water surface.[19] From stabilization experiments and an Avrami analysis we concluded that the water surface crystallization process could be described by an activated nucleation followed by a one-dimensional growth of the nuclei, during which the helices are lined up in a parallel way so as to optimize their lateral contacts: the crystallites would then grow mainly in the direction perpendicular to the helix axes. We can explain the reversal of the observed lateral orientation if we assume that the rigid

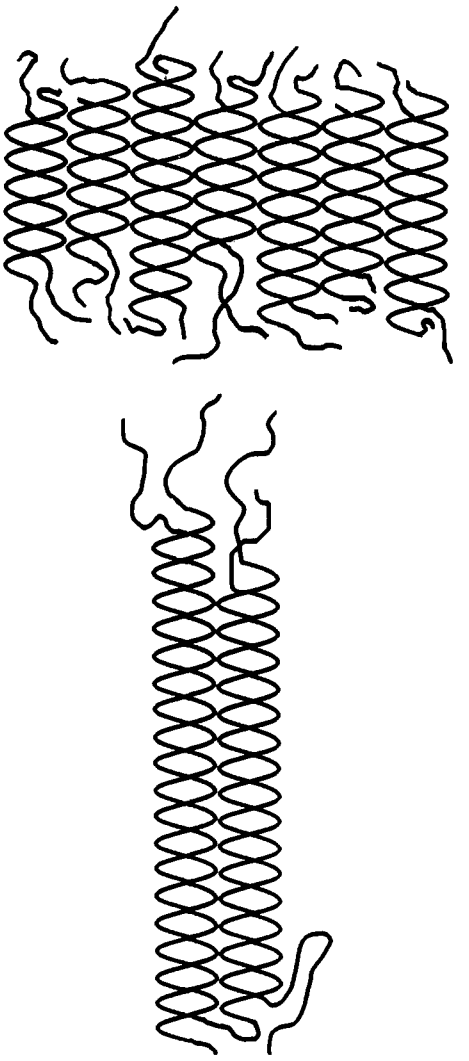

Figure 11. Schematic representation of water surface crystallites of isotactic PMMA. Top: shape as suggested for low molecular weight samples. Bottom: shape as suggested for high molecular weight samples. The suggested differences are exaggerated for clarity.

structures that may be oriented in a flow field are not isolated (double) helices but are in fact the surface crystallites that the helices are part of. These crystallites will be oriented in the dipping direction during transfer, but this process will depend strongly on the *aspect ratio* of the crystallites. For crystallites that have aspect ratios of approximately 1, the crystallites will be oriented more or less randomly. If the crystallites are small (consisting of few helices), the longest axis of the crystallite will coincide with the helix axis. If, on the other hand, the crystallites consist of many parallel helices, the longest axis may be perpendicular to the helix axis (Figure 11). Since the longest axis of the crystallites will be oriented in the dipping direction, this will correspond to an orientation of the *helices* perpendicular to this dipping direction. An increase in the aspect ratio of the crystallites will increase the average extent of their lateral orientation.

If the surface crystallization is to occur at low surface pressures (e.g., 6.5 mN/m), the critical nucleus size will be relatively large because of the rather low driving force for helix formation. Therefore the nucleation rate might be low, leading to large crystallites to be formed; because of the one-dimensional character of the growth this corresponds to *broad* crystallites. Surface crystallization at higher surface pressures would be characterized by a higher nucleation density and result in small, narrow crystal-

lites. This may explain the difference between the 6.5 and 12 mN/m stabilized monolayers.

For the materials that have rather low molecular weights, it can also be anticipated that the nucleation process at the water surface is suppressed, because they approach the critical chain length for helix formation under these conditions, so that the gain in free energy per helix formed will be lower, leading to a larger critical nucleus size, and consequently a lower nucleation rate and nucleation density. This lower nucleation density may eventually lead to broader crystallites, consisting of helices of lengths that are limited by the molecular weight. Higher molecular weight fractions will not suffer from this suppression of the nucleation rate, so that the higher nucleation rate may result in narrower crystallites. This explanation appears to be compatible with all lateral orientation effects observed.

Mixing of the isotactic PMMA with a molecular weight of 36 000 with an amount of the material of 2800 molecular weight also produces deviating values for $L_{C=O}$: using mixtures with a weight fraction of $\bar{M}_n$ 2800 material of 26% and 45% produces multilayers (stabilization and transfer at 12 mN/m) in which the preference of the helices parallel to the dipping direction has disappeared, and even small negative $L_{C=O}$ values are observed. Probably also in these cases, the nucleation is suppressed by the presence of the low molecular weight component that does not participate in the helix formation. This is also indicated by the pressure–area isotherms of these mixtures.[19]

The lateral orientation of the crystalline structure in the thin film can thus be controlled by the molecular weight composition as well as the monolayer stabilization pressure.

Conclusions

From infrared measurements it was deduced that at 12 mN/m surface pressure Langmuir–Blodgett films of isotactic PMMA are transferred in a crystalline-like conformation, presumably a (double) helical structure, whereas at low surface pressures the monolayer is deposited in a more or less random conformation. Support for these hypotheses was found before in the monolayer behavior of isotactic PMMA.[19]

The Langmuir–Blodgett layers transferred at high surface pressures can easily be crystallized, in sharp contrast to the normal behavior of amorphous isotactic PMMA, requiring a very time-consuming crystallization process, especially in thin films. In the crystal structure formed in the thin film, the helices strongly tend to lie parallel to the substrate. In the XY plane (parallel to the surface) strong orientational effects can also be observed that are controlled by the molecular weight of the polymer and its water surface crystallization history. The aspect ratio of the water surface crystallites appear to determine the lateral orientation of the multilayers. Almost unidirectionally oriented highly crystalline thin films can be prepared this way.

These crystalline polymer thin films may also be interesting from an application point of view (optics, microlithography) because of the easily controllable anisotropy of several properties.

Appendix 1: Effect of the Film Density on IR Spectra

Variations of the density of the deposited layers were taken into account in the spectral simulations by a simultaneous adjustment of the layer thickness and its optical constants. The thickness is adjusted so that the total amount of material in the film remains constant:

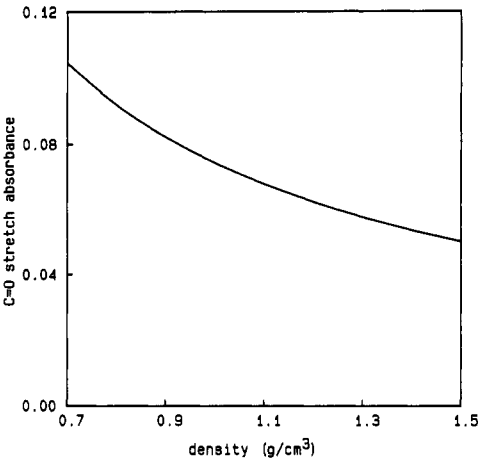

Figure 12. Calculated maximum C=O stretch absorbance for a 200 Å (ρ_n 1.2 g/cm³) film of isotactic PMMA, as a function of density (with simultaneously adjusted film thickness; see text).

the thickness is assumed to be inversely proportional to the density. The optical constants of material with a deviating density were estimated on the basis of the Lorentz-Lorentz equation:[38] a linear relation between the polarizability per unit volume and the density was assumed. The optical constants can then be calculated by

$$(\mathbf{n}^2 - 1)/(\mathbf{n}^2 + 2) = (\rho/\rho_n)((\mathbf{n}_n^2 - 1)/(\mathbf{n}_n^2 + 2))$$

with ρ and ρ_n representing the densities under actual and "normal" conditions, respectively, and with $\mathbf{n}$ and $\mathbf{n}_n$ being the complex refractive indices under actual and "normal" conditions, respectively.

The reflection spectra of the films deposited on gold substrates and also the transmission spectra of thin films on IR-transparent substrates can be calculated to be sensitive to changes in the density of the film. For grazing incidence reflection spectra on gold (80° angle of incidence, specular setup, parallel polarization) the major effect of a changing density of the film is the change in absolute intensity observed over the whole spectrum: lower densities result in significantly higher absorption values, higher densities in lower absorption values (note that the total amount of material in the film is kept constant!). The shape of the spectrum (relative peak heights, peak positions), however, does not change very much upon varying the density. This variation of the thin film absorption with film density may be an important complication for a direct quantitative interpretation of GIR spectra.

In Figure 12 the calculated maximum intensity of the carbonyl stretching vibration (GIR on gold, 80° angle of incidence, parallel polarization, "normal" film thickness 200 Å at a standard density of 1.2 g/cm³) is shown as a function of density.

For transmission experiments of thin polymer films on ZnS and Si substrates an effect of the density of the polymer films can also be anticipated: in contrast with the grazing incidence reflection experiments, the films with the highest densities will absorb IR radiation more strongly as compared to film of lower densities, the total amount of material being equal. The density effect on the absorption is not as strong as for the grazing incidence reflection experiments.

Appendix 2: Dichroism of Helical Structures

The absorption intensity of vibrations is known to be proportional to the average value $\langle \cos^2 \vartheta \rangle$, ϑ being the angle between the electrical field vector and the dipole

transition moment associated with the vibration. If we consider a vibration localized in a functional group, fixed in a helical structure, the value of $\langle \cos^2 \vartheta \rangle$ can easily be evaluated by assuming that the dipole transition moments will be distributed in a cylindrically symmetrical way along the helices, so that $\cos^2 \vartheta$ can be averaged over all positions obtained after rotating the helix over an arbitrary angle. Thus, $\langle \cos^2 \vartheta \rangle$ is determined by the angle between the dipole moments and the helix axis ϕ, and the orientation of the helices with respect to the electrical field associated with the IR radiation. For helices lying parallel to a substrate (in the XY plane), $\langle \cos^2 \vartheta \rangle = 0.5 \sin^2 \phi$ for an electrical field vector perpendicular to this substrate (along the z axis, the GIR situation), independent of the orientation of the helices within the XY plane. This results in a relative enhancement of the absorptions associated with vibrations having a dipole transition moment with ϕ larger than 55°, as compared to a randomly oriented structure ($\langle \cos^2 \vartheta \rangle = {}^1/_3$), and a similar suppression of absorptions by vibrations with a ϕ smaller than this value. For transmission experiments, the same situation will lead to values for $\langle \cos^2 \vartheta \rangle$ of 0.5–0.25 $\sin^2 \phi$ for unpolarized IR radiation, or in the case of randomly oriented helical structures for either polarization. For perfectly unidirectionally oriented helical structures, $\langle \cos^2 \vartheta \rangle = \cos^2 \phi$ for a polarization parallel to the helix axes and $\langle \cos^2 \vartheta \rangle = 0.5 \sin^2 \phi$ for the polarization perpendicular the helix direction.

References and Notes

(1) Kuan, S. W. J.; Frank, C. W.; Fu, C. C.; Allee, D. R.; Maccagno, P.; Pease, R. F. W. *J. Vac. Sci. Technol. B* **1988**, *6*(6), 2274.
(2) Kimura, F.; Umemura, J.; Takenaka, T. *Langmuir* **1986**, *2*, 96.
(3) Allara, D. L.; Nuzzo, R. G. *Langmuir* **1985**, *1*, 52.
(4) Allara, D. L.; Swalen, J. D. *J. Phys. Chem.* **1982**, *86*, 2700.
(5) Rabolt, J. F.; Burns, F. C.; Schlotter, N. E.; Swalen, J. D. *J. Chem. Phys.* **1983**, *78*, 946.
(6) Naselli, C.; Rabolt, J. F.; Swalen, J. D. *J. Chem. Phys.* **1985**, *82*, 2136.
(7) Bohn, P. W. *Spectroscopy* **1988**, *3*, 38. Allen, S. *Inst. Phys. Conf. Ser. No. 103: Section 2.3* **1989**, 163.
(8) Stroeve, P.; Srinivasan, M. P.; Higgins, B. G.; Kowel, S. T. *Thin Solid Films* **1987**, *146*, 209.
(9) Ringsdorf, H.; Schmidt, G.; Schneider, J. *Thin Solid Films* **1987**, *152*, 207. Elbert, R.; Laschewsky, A.; Ringsdorf, H. *J. Am. Chem. Soc.* **1985**, 107, 4134.
(10) Arndt, T. Thesis, Max Planck Institut für Polymerforschung, Mainz, BRD, 1988.
(11) Nakahara, H.; Fukuda, K. *J. Colloid Interface Sci.* **1979**, *69*, 24.
(12) Takenaka, T.; Nagami, K.; Gotoh, H.; Gotoh, R. *J. Colloid Interface Sci.* **1971**, *35*, 395.
(13) Golden, W. G.; Snyder, C. D.; Smith, B. *J. Phys. Chem.* **1982**, *86*, 4675.
(14) Chollet, P. A.; Messier, J.; Rosilio, C. *J. Chem. Phys.* **1976**, *64*, 1042.
(15) Duda, G. Thesis, Max Planck Institut für Polymerforschung, Mainz, BRD, 1988.
(16) Francis, S. A.; Ellison, A. H. *J. Opt. Soc. Am.* **1959**, *49*, 131.
(17) Greenler, R. G. *J. Chem. Phys.* **1966**, *44*, 310.
(18) Chatzi, E. G.; Urban, M. W.; Ishida, H.; Koenig, J. L.; Laschewski, A.; Ringsdorf, H. *Langmuir* **1988**, *4*, 846.
(19) Brinkhuis, R. H. G.; Schouten, A. J. *Macromolecules*, preceding paper in this issue.
(20) Graf, R. T.; Koenig, J. L.; Ishida, H. *Appl. Spectrosc.* **1985**, *39*, 405.
(21) Ohta, K.; Ishida, H. *Appl. Spectrosc.* **1988**, *42*, 952.
(22) Abelès, F. *Ann. Phys.* **1948**, *3*, 504.
(23) Allara, D. L.; Baca, A.; Pryde, C. A. *Macromolecules* **1978**, *11*, 1215.
(24) *Handbook of optical constants of solids*; Palk, E. D., Ed.; Academic Press: New York, 1985.
(25) Belopolskaya, T. V. *Vysokomol. Soyed.* **1972**, *A14*, 640. Belopolskaya, T. V. *Vysokomol. Soyed.* **1971**, *A13*, 1119.
(26) O'Reilly, J. M.; Mosher, R. A. *Macromolecules* **1981**, *14*, 602.
(27) Havriliak, S.; Roman, N. *Polymer* **1966**, *7*, 387.
(28) Lipschitz, I. *Polym.-Plast. Technol. Eng.* **1982**, *19*(1), 53.
(29) Kusanaga, H.; Tadokoro, H.; Chatani, Y. *Macromolecules* **1976**, *9*, 531.
(30) Bosscher, F.; Ten Brinke, G.; Eshuis, A.; Challa, G. *Macromolecules* **1982**, *15*, 1364.
(31) Dybal, J.; Krimm, S. *Macromolecules* **1990**, *23*, 1301.
(32) De Boer, A.; Alberda van Ekenstein, G. O. R.; Challa, G. *Polymer* **1975**, *16*, 930.
(33) Könnecke, K.; Rehage, G. *Colloid Polym. Sci.* **1981**, *259*, 1062.
(34) Brinkhuis, R. H. G., Schouten, A. J., to be published.
(35) Billon, N.; Haudin, J. M. *Colloid Polym. Sci.* **1989**, *267*, 1064.
(36) Takeda, F.; Matsumoto, M.; Takenaka, T.; Fujiyoshi, Y.; Uyeda, N. *J. Colloid Interface Sci.* **1983**, *91*, 267 and references therein.
(37) Schoondorp, M. A.; Vorenkamp, E. J.; Schouten, A. J., submitted to *Thin Solid Films*
(38) Huglin, M. B., Ed. In *Light Scattering from Polymer Solutions*; Academic: New York, 1972; p 35.

Registry No. i-PMMA, 25188-98-1.